Mechanical Engineering Research; Vol. 3, No. 1; 2013
ISSN 1927-0607 E-ISSN 1927-0615
Published by Canadian Center of Science and Education

Bridge Concept Design Using Heuristic Fuzzy Optimum Design and FEM

Heikki Martikka[1] & Erkki Taitokari[2]

[1] Himtech Oy, Engineering, Ollintie 4, Joutseno, Finland

[2] Oy Scan Fibre Ltd., Liisakatu 26, Imatra, Finland

Correspondence: Heikki Martikka, Himtech Oy, Engineering, Ollintie 4, Joutseno FIN-54100, Finland. Tel: 358-40-839-3167. E-mail: heikki.martikka@pp.inet.fi

Received: November 25, 2012 Accepted: December 21, 2012 Online Published: January 20, 2013

doi:10.5539/mer.v3n1p44 URL: http://dx.doi.org/10.5539/mer.v3n1p44

This research is financed by Himtech Oy and Oy Scan Fibre Ltd.

Abstract

In this study the aim is to present results of bridge concept design using heuristic fuzzy optimum design and FEM. The bridge concept is chosen as the basic suspension type. The deck plate rests on four supports. The middle supports are towers with suspension cables to lift up the bridge plate for minimising its deflection and bending stresses. Mass distribution load and flutter loading act on the plate. Geometric design variables are topology and dimensions of cables and deck. Material variable options are low strength and high strength steel. Decision variables are based on design variables. The main ones are cost and safety factors. The total goal is maximization of the fuzzy satisfaction of the user on all decision variables. The same optimal geometry is obtained for both steel options giving nearly equal performance. The softer steel option is preferable due lower cost. The model and FEM results agree reasonably in stresses and deflections. The fuzzy model used is shown to be an extension of probabilistic models.

Keywords: suspension bridge, fuzzy optimum design, probabilistic design

1. Introduction

According to the traditional design philosophy bridges are needed only as means to get across some gap, like those between buildings and terrain valleys and rivers. They are subjected to traffic and environmental loads ranging from winds to corrosive rains, floods, thermal loads, solar radiation and seismic loads.

Materials range from wood, steel and concrete. The need of obtaining reliable long service life can be satisfied by continuous real time condition monitoring and self healing capability.

The bridge design goal can also be expressed easily as fuzzy satisfaction of the end user. This optimum fuzzy approach to solve a concept design is used and discussed by (Martikka & Pöllänen, 2010). This method is based on results of (Diaz, 1988). At each bridge there are crucial locations where the safety factors should be high enough .Structural mechanics and statics are needed to obtain analytical model to define first the design variables and based on them the decision variables. Satisfactions are the defined on them. Now the bridge design is considered starting from heuristic concept design.

Structural analysis by (Case et al., 1993; Boresi, 1993) are considered. Flow induced vibration and flutter are important in bridges as by (Blevins, 1990) and by (Dimarogonas, 1992). Theory of plates is considered by (Ventsel et al., 2001) and (Szilard, 1975). Bridge design codes are described by (Merritt, 1983).

In this study the advanced FEM NX Nastran is applied. A short survey of the design history of bridges shows that the basic concept was used in the ancient Yaxchilan bridge (Yaxchilan), (Chiaopas) thousands years ago and Chakzam (Cable stayed bridges) bridge in 1430. Their design methods are not known to us. The Brooklyn Bridge (Brooklyn Bridge) in 1883 is similar. The Tacoma (Tacoma) bridge in 1940 was structurally similar but flexible. Now bridges are built with span over 2 kilometres.

The present day goals emphasise need to get also ecological and ecoenergy benefits from bridges. Bridges are subjected to energetic air and water flow loads and to solar energy and temperature difference loads. The task of bridges could be not only to resist loads but convert them to useful electricity using wind powers generators and solar panels at bridges. The trend is that longer utilisation times are required and also ecoenergy profit from these very large investments.

2. Bridging a Chasm Concept Survey

The bridge design activity may be logically presented as design loop shown in Figure 1.

2.1 The Design Loop as Formalising the Activity of Design and Manufacturing Work to Satisfy Needs

The design loop in Figure 1 is applied to the task of realisation of a bridge. It starts from a need of end users to get a safe and low cost passage over a chasm. History shows that a need for bridging is initiated at location where some chasm or river separates a population which needs transit interconnections.

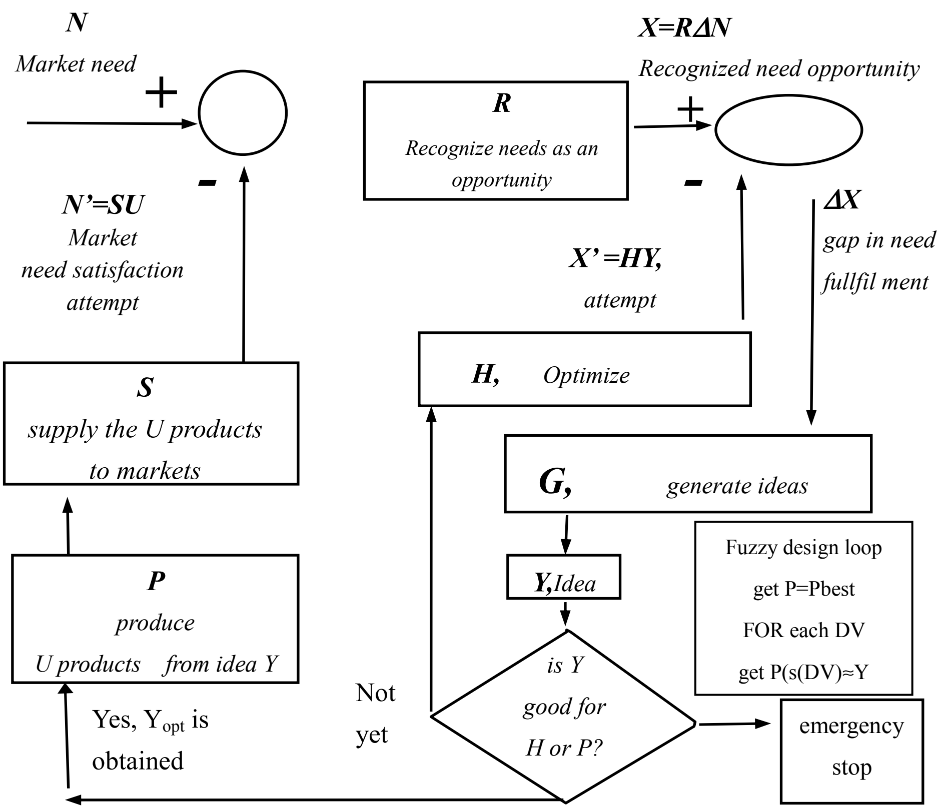

Figure 1. A typical design control loop for innovation tasks

From this control loop the equation for the optimal design concept is solved as

$$Y_{\text{opt}} = \frac{GR}{1 + GH + GR \cdot SP} \cdot N \quad (1)$$

Market survey recognition may be estimated as a factor of efficiency R = 0.7. First one may desire just one optimal and successful product concept, Y_{opt} =1. This is obtained when assuming G = 100 concepts are generated by the fuzzy design loop program. Then the optimal concept is selected from them with resulting in selection fraction H =1/100. This is chosen as the one Y to be produced P times. The number of prototype products U = PY = 100. From these one is made and supplied to markets to satisfy markets, S = 1. The need is N and N' is the attempt to satisfy N. Production is thus equal to N and the market need is satisfied.

$$\begin{aligned} &One.optimal.concept \quad Y \Rightarrow 1 \Rightarrow \\ &N = needed. \Rightarrow Y = 1.is.P = produced \Rightarrow S = 1.is.\text{sup}\,plied \\ &N' = products.to.market \quad N' = SPY = 1 \cdot P \cdot 1 \quad \Rightarrow full.satisfaction \quad N = N' = P \end{aligned} \quad (2)$$

Using these one obtains one optimal concept.

$$Y_{\mathrm{opt}} = \frac{100 \cdot 0.7}{1 + 100 \cdot 0.01 + 100 \cdot 0.7 \cdot 1 \cdot P} \cdot N = \frac{70}{2 + 70 \cdot P} \cdot N \approx \frac{N}{1.03P} \Rightarrow 1 \Rightarrow P \approx N \tag{3}$$

2.2 Innovation of Alternative Solutions to Satisfy the Bridging Need

According to (Kozak, Roberts, 1983) bridges are classified in two types: fixed and movables.

There are many alternatives. Some are shown in Figures 2 and 3.

2.2.1 Bridging Over Chasm with a Static Structure or the Classical Bridge

Several alternatives are shown in Figure 2.

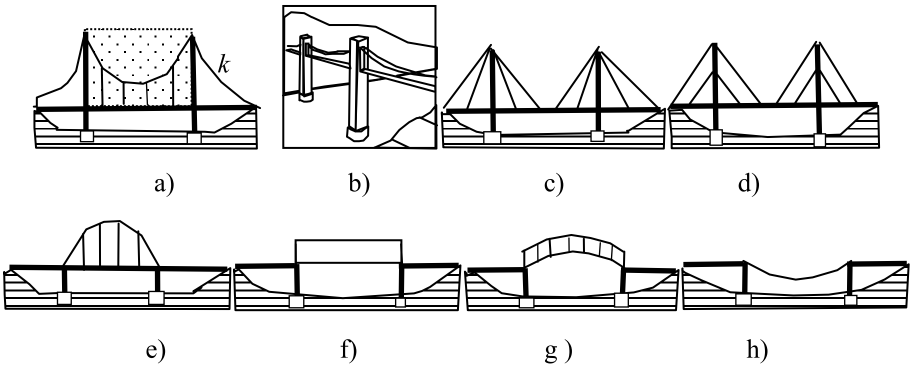

Figure 2. Bridge types. a) Suspension bridge; b) Schematic reconstruction picture; c) Cable stayed bridge of fan type; d) Cable stayed bridge of harp type; e) Parabolic form analogous to constant edge stress beam; f) Straight stiff beam bridge; e) Arch form; h) Only cable with small bending resistance

2.2.2 Bridging over a Chasm with Various Means

The function of a stationary bridge is restricted to allow passage over a chasm. The bridging function may be satisfied by other means. Some possibilities are sketched in Figure 3.

a) Cable trolley moves above the chasm in air.

b) Ferry moves in the water by guided by cables.

c) Boat moves on water.

d) Tunnel below the chasm.

e) Aircraft type transport over chasm.

f) Movable bridge deck allowing passage of ships across the bridge.

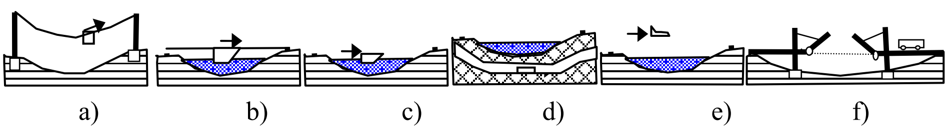

Figure 3. Bridging over chasm with various means

2.3 Famous Historical Suspension Bridges

Bridges are old inventions.

2.3.1 Yaxchilan Bridge in Mexico and Chakzam Bridge in Lhasa

Figure 4 shows an artistic reconstruction of the bridge built by the Maya civilisation (from 1800BC to 900AD) with length 200 meters (Yaxchilan). The Chakzam bridge (Cable stayed bridges) was built in 1430AD in Lhasa with cables suspended between towers and vertical suspender cables carrying the weight of a planked footwear below.

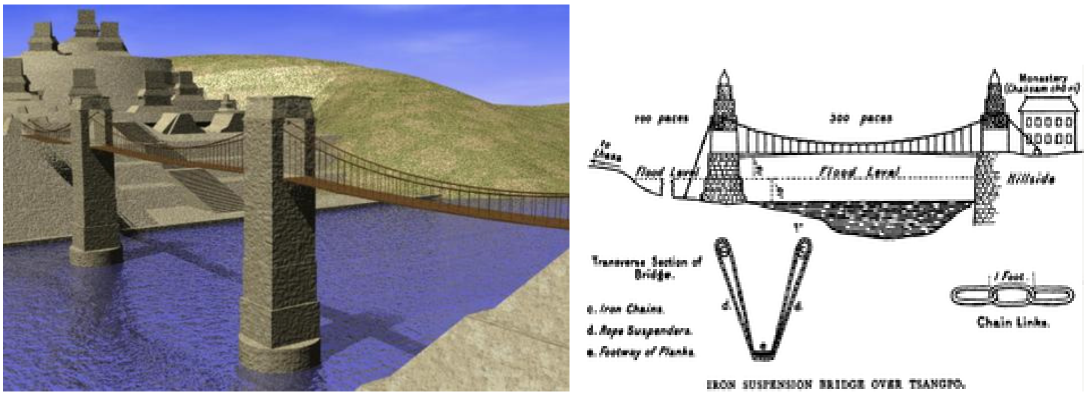

a) b)

Figure 4. a) Pictorial reconstruction of the ancient Yaxchilan Bridge in Mexico (Yaxchilan, Chiaopas); b) The Chakzam bridge was built in 1430AD in Lhasa. Both are topologically similar, Cable-stayed bridges

2.3.2 The Tacoma Narrows Bridge Built in 1940

This was opened in 1940 (Tacoma) but collapsed due to aero elastic flutter four months later, Figure 5a. The design is twin suspensions with longest span L = 853 m.

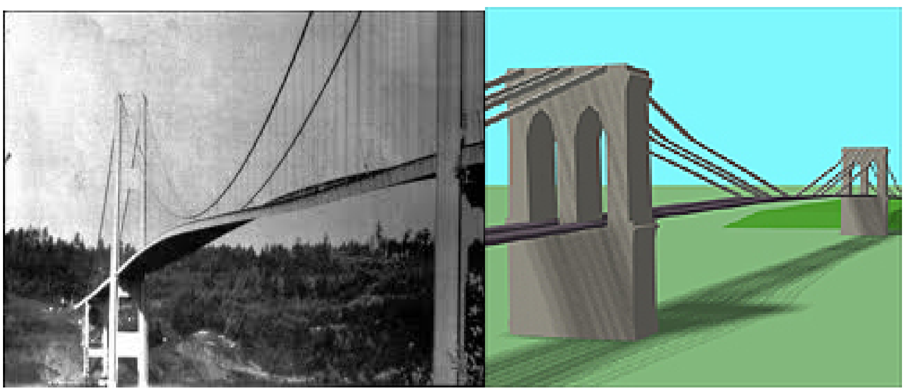

a) b)

Figure 5. Suspension bridges. a) The Tacoma Narrows bridge in 1940 before failure by flutter (Tacoma) The span is L=853m. b) Sketch of the support principle of the Brooklyn Bridge built in 1883 (Brooklyn Bridge). The span is L=486m

2.3.3 The Brooklyn Bridge Built in 1883

The Brooklyn Bridge suspension principle is shown in Figure 5b. (Brooklyn Bridge) The suspension cables are the first in major bridges to use steel wire. It corrodes much faster than the previously used wrought iron. The corrosion protection was made by galvanising.

2.4 Classical Bridge Engineering

Ancient bridge design codes are not known to us. Modern bridge design is based on advances in mechanics and material science. The classical bridge engineering is discussed by (Kozak & Roberts, 1983). They give a definition: “bridge engineering covers the planning, design construction, and operation of structures that carry facilities for movement of humans, animals, or materials over natural or created obstacles.”

In this study the aim is to survey some aspects affecting the success of bridge design measured with statistics.

Bridges must support many loads and have a reliably long useful life time with low maintenance costs.

(L1) Dead load including permanent utilities

(L2) Live load L and impact I

(L3) Longitudinal forces due to acceleration or deceleration and friction F

(L4) Centrifugal forces. Due to vehicles driving in curved bridges

(L5) Wind pressure acting on the structure Q and moving load WL

(L6) Earthquake forces EQ

(L7) Earth pressure E, water and wind pressure ICE, stream flow SF, and uplift B acting on the substructure

(L8) Forces from elastic deformations including rib shortening R

(L9) Forces from thermal deformations T including shrinkage S

This list does not include specifically environmental loads, corrosion, corrosion fatigue, and creep and radiation deterioration. All these reduce the strength while loads are increasing. The result is that factors of safety become too low against overloads like crashes against bridges, earthquakes, high river and wind flows. The failure statistics shows that generally the bridges have been under designed at safety critical locations.

All these loads and their interactions need to be included in the optimum design.

2.5 Reliability Based Design Approach

This approach may be applied using results by (Dhillon & Singh, 1981) and (Leitch, 1988). A simplistic application is shown in Figure 6.

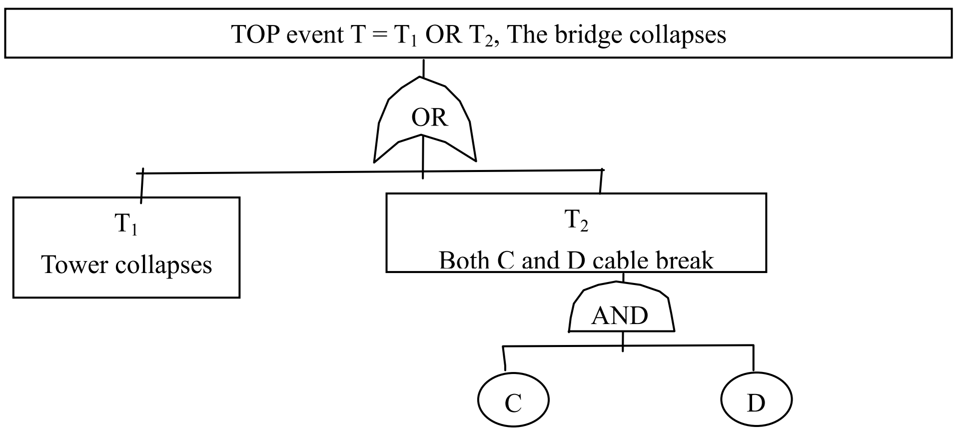

Figure 6. Analysis of top event using fault tree method

The top event T is the collapse of the bridge. The failure histories show that impacts and overloading on too weak structures have caused most failures. This may be the T_1 event. Now for simplicity the second event T_2 is failure of main C and D cables. Using Boolean logic the top event is

$$T = T_1 + T_2 = T_1 + C \cdot D, T_2 = C \cdot D \tag{4}$$

The probabilities of the basic events are tentatively estimated as

$$\begin{gathered} P(T_2 = C \cdot D) = P(C) \cdot P(D) = 0.006 \cdot 0.007 \\ P(T_1) = 0.005, P(C) = 0.007, P(D) = 0.006 \end{gathered} \tag{5}$$

The probability of the top event is

$$\begin{gathered} P(T) = P(T_1 + T_2) = P(T_1) + P(T_2) - P(T_1)P(T_2) \\ P(T) = 0.005 + 0.006 \cdot 0.007 - 0.005 \cdot 0.006 \cdot 0.007 \approx 0.005 \end{gathered} \tag{6}$$

This shows that overloading on too weak bridges is the dominant risk. This is supported by statistics.

This study emphasises the emerging need that the reliable utility of bridges to the society should be increased due to the high investment costs of bridges.

2.6 Bridges as Harvesters of Ecoenergy

Traditional goal is the narrow utilitarian aim to offer a bridging service and collect taxes. Bridge taxes could be levied from the environment. The old design goal was only to passively resist all kinds of energy flows from winds to water flow below and solar radiation and mechanical vibrations. Instead of resisting their energy flows may be harvested and converted to produce ecologically electric energy for the bridge maintenance and the society. Since there are many bridges the total obtained power may be high.

Annual average wind power may be about 0.2 times the maximal power as given by (Ackermann & Söder, 2000)

$$P_{max} = \tfrac{1}{2}\rho A\overline{v}^3 C_{P,Betz} \Rightarrow \tfrac{1}{2}1.2\tfrac{kg}{m^3}\cdot 100m^2\cdot\left(10\tfrac{m}{s}\right)^3 0.59 = 35kW, P_{avarage} = 0.2P_{max} = 7kW$$
$$C_{P,Betz} = 0.59,\ A = 100m^2,\ \overline{v} = 10\tfrac{m}{s},\ N = 10\tfrac{windmills}{1\,bridge},\ P_{total} = 70kW \tag{7}$$

Solar power may be harvested with a solar panel area about N_s=500 panels of one square meter area. The annual averaged power maybe P_s=0.1 kW yearly giving power $P_{solar}=N_s{\cdot}P_s$=50kW. The power may be used to lighting, heating, maintenance and monitoring of the bridge.

The total average wind and solar power from a moderate size bridge may be even 0.2MW. There may be about 1000 such eco-energy bridges producing 200MW.

3. The Studied Structure

The present goal is to study bridge design heuristics. A simplified bridge concept is chosen as shown in Figure 7.

3.1 Geometry and Materials

The geometry is shown in Figure 7. The span is L = 2a+b. Materials of cables and deck are steel options shown in Table 1.

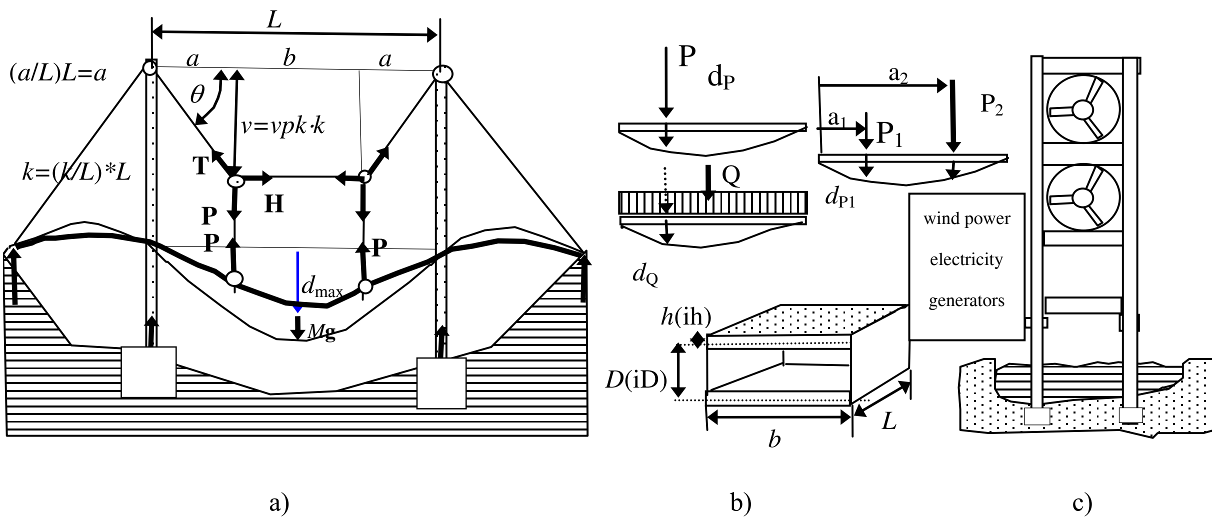

Figure 7. The structure studied. a) The geometrical design variables cable and support tower geometry
b) Deflection models and deck dimensions. c) Bridge as econergy harvester

3.2 Function of a Bridge

Conventionally a bridge is conceptually defined as an immobile structure affording a passage of objects contacting the bridge over a chasm. End user satisfaction on the bridge is high with safe and comfortable passage.

3.3 Forces and Moments

The cables are loaded under tension and the bridge deck load is bending moment. Force balances at the cable node gives, Figure 7

$$\begin{aligned}\Sigma F &= T + H + P = 0\\ \Sigma F_x &= -T\cos\theta + H = 0\\ \Sigma F_y &= +T\sin\theta - P = 0\end{aligned} \tag{8}$$

From these the forces *H* and *T* can be expressed depending on the *P* force

$$H = \frac{P}{tan\,\theta} \quad ,\sigma_H = \frac{H}{A_H} \quad ,\sigma_P = \frac{P}{A_P} \tag{9}$$

The *T* force is

$$T = kf_{\mathrm{T}} = k\cdot t\left(\frac{1}{\cos\theta} - 1\right) = \frac{P}{\sin\theta}, \sigma_{\mathrm{T}} = \frac{T}{A_{\mathrm{T}}} \tag{10}$$

The cable topology determines the force ratios. The *H* force is obtained from this ratio

$$\frac{P}{H} = tan\,\theta = \frac{v}{a} \Rightarrow \frac{\left(\frac{v}{k}\right)\left(\frac{k}{L}\right)}{\left(\frac{a}{L}\right)} \Rightarrow v = \left(\tfrac{v}{k}\right)k, k = \left(\tfrac{k}{L}\right)k, a = \left(\tfrac{a}{L}\right)L \tag{11}$$

This suggests use of relative dimensionless variables in design. The factors of safety are

$$N_T = \frac{\sigma_{all}}{\sigma_T} \quad N_H = \frac{\sigma_{all}}{\sigma_H}, \quad N_P = \frac{\sigma_{all}}{\sigma_P} \tag{12}$$

The moments at the bridge plate are discussed in the Appendix 1.

4. Fuzzy Goal Formulation Using Decision Variables

The design variable vector **x** = (load functions, geometry, materials) elements are not goals in themselves.

From these it is necessary to form decision variable event **s** = (cost, factors of safety...) = **s**(**x**). But even this is not the goal that would satisfy the end-user unequivocally and ambiguously. End-user goals are often vague and fuzzy. They can be defined fuzzily as maximisation of total customer satisfaction on it (Diaz, 1988).The total event is decision variable *s* and it is intersection of decision variables s_{k}

$$s = s_1 \cap s_2 \cap s_3 \cap s_4 \cap s_5 \cap s_6 \tag{13}$$

The design goal is maximisation of the total satisfaction of the customer on the product

$$P(s) \Rightarrow P(s) = P(s_1)\cdot P(s_2)\cdot \ldots\ldots \cdot P(s_{\mathrm{n}}), Q = \max P \tag{14}$$

Now all goals and constraints are formulated consistently by one standard flexible fuzzy function. This is illustrated in Figure 8.

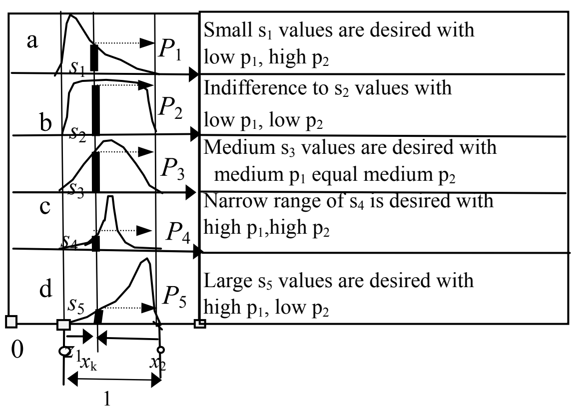

Figure 8. The distribution form and skewness are determined by the bias parameters

In appendix 3 a mechanistic analytic model is presented for the bias parameters.

5. Design Variables

5.1 Material Design Variables

Steel option design variables are shown in Table 1.

Table 1. Material variables. The Paris law *C* and *m* parameters are calculated with Gurney's (Gurney, 1978) model

	OX steel im = 1	St52 steel im=2
Yield strength (MPa)	Re(1) = 1000	Re(2) = 335
Tensile strength (MPa)	Rm(1) = 1100	Rm(2) = 520
unit cost (eur/kg)	Cm(1) = 20	Cm(2) = 5
density (kg/m^3)	rho(1) = 8000	rho(2) = 8000
ecological value	eco(1) = .1	eco(2) = .7
corrosion resistance	corres(1) = .8	corres(2) = .15
Elastic modules (MPa)	E(1) = 205000	E(2) = 205000
Threshold intensity(Nmm$^{-3/2}$)	Kth(1) = 275	Kth(2) = 190-144 · Rs
Initial crack size (mm)	$a_0(1) = 1$	$a_0(2) = 1$
Paris C parameter	C(1) = 4.64E-12	C(2) = 1.67E-14
Paris m exponent	m(1) = 2.52	m(2) = 3.36

Stress ratio $R_s = \sigma_{min}/\ \sigma_{min} = 0$, K_{th} (N·mm$^{3/2}$)

5.2 Functional Design Variables and Parameters

The cable load P was varied as a design variable. Other forces depend on it.

Table 2. The cable load PP(iP). Actual used = P(iP) = PP(iP)·xp. Optimal scaling factor xp = 10

PP(iP) (kN)	10	20	30	40	50	60	70	80	100
iP	1	2	3	4	5	6	7	8	9

The load force *Q* on the deck area *bL* is due to pressure *p*, *Q*=*p b L* = 5000*10*200 = 10MN.

5.3 Geometrical Design Variables

Independent and discrete geometrical variables are from the options listed in Table 3.

Table 3. Geometrical design variables options

index k	Cable area AA(iA)* 10^6*mm^2 A=xa*AA	Bridge plate thickness *hh*(ih) (m) h= xh*hh	Bridge plate separation DD(iD) D=xD*DD	ratio *kkpL*(ih) =k/L(m) k=(k/L)L	Ratio vpk=v/k v=(v/k)k	Ratio aapL= aa/L a=(aa/L)L
1	100	0.01	0.24	0.2	0.1	0.15
2	200	0.02	0.28	0.24	0.15	0.2
3	300	0.03	0.30	0.28	0.20	0.3
4	400	0.04	0.32	0.30	0.3	0.35
5	500	0.05	0.36	0.34	0.4	0.40
6	600	0.06	0.38	0.38	0.5	0.42
7	700	0.07	0.42	0.4	0.6	0.44
8	800	0.08	0.45	0.45	0.7	0.45
9	1000	0.10	0.50	0.50	0.8***	0.48

Here the input list vector may be zoomed with suitable scaling factors.

$$\begin{aligned} &A(iA) = x_a \cdot AA(iA), \quad x_a = 2 \\ &h(ih) = x_h \cdot hh(ih), \quad x_h = 1 \\ &D(iD) = x_D \cdot DD(iD), \quad x_D = 0.2 \\ &kpL(ikpL) = x_k \cdot kkpL(ikpL), \quad x_k = 0.5 \end{aligned} \tag{15}$$

5.4 Decision Variables for Defining Goals

Decision variables s(k) depend on the design variables x(i).

5.4.1 Goal of Obtaining Low Cost K or Decision Variable S_1

Cost is now material cost of the bridge and cables. The masses are

$$\begin{aligned} &m_T = \rho A_T L_T = \rho A_T \frac{a}{\cos\theta}, \quad ,L_T = \sqrt{a^2 + v^2}, \quad m_H = \rho A_H L_H = \rho A_H b \\ &m_B = \rho_B A_B L_B = \rho A_H (2a + b), \quad L_B = L = given, \quad m = m_B + m_Q, \quad m_Q = \frac{Q}{g} \end{aligned} \tag{16}$$

Here m_B is the mass of the bridge, m_Q is the load Q mass, m is total mass of the mid deck plate. Both sides are included with N_{side} =2.

$$K = c(im) N_{side} (2m_T + 2m_P + m_H) + c(im_B) m_B \tag{17}$$

The desired range of cost K is defined using a suitable scaling cost K_{max}

$$s_1 = xK = \frac{K}{K_{max}} \quad , \quad Range = 0.01 < s_1 < 50, \quad p_1, p_2 = 0.1, 3 \tag{18}$$

5.4.2 Goal of Obtaining Satisfactory Factor of Safety N_{yT} for the T cables

The aim is to prevent plastic yielding with maximal static stress or decision variable s_2.

Now the dynamic effects are not considered.

$$s_2 = N_{yT} = \frac{S_y}{\sigma_T}, \quad \sigma_T = \frac{T}{A_T(iA)} \quad 2 < s_2 < 100 \quad p_1, p_2 = 1, 1 \tag{19}$$

5.4.3 Goal of Obtaining Satisfactory Factor Safety N_{yP} for the P Cables

The aim is to prevent plastic yielding with maximal static stress.

$$s_3 = N_{yP} = \frac{S_y}{\sigma_P}, \sigma_P = \frac{P}{A_P(iA)} 2 < s_3 < 100 \quad p_1, p_2 = 0.1, 1 \tag{20}$$

5.4.4 Goal of Obtaining Satisfactory Factor Safety N_{yH} for the H Cables

The aim is to prevent plastic yielding with maximal static stress.

$$s_4 = N_{yH} = \frac{S_y}{\sigma_H} \quad , \quad \sigma_H = \frac{H}{A_H(iA)} \quad 2 < s_4 < 100 \quad p_1, p_2 = 1, 1 \tag{21}$$

5.4.5 Goal of not Exceeding the Crack Threshold

The threshold crack length depends on the magnitude of the peak stress range

$$a_{th0}(im) = \frac{1}{\pi}\left[\frac{\Delta K_{th}}{Y\Delta\sigma}\right]^2, \Delta\sigma = \sigma_{max} - \sigma_{min} = 0.2\sigma_P \tag{22}$$

The stress increasing factor may come from many sources and they may be superposed.

The total dynamic load factor is estimated in appendix 2.

$$Y = K_t K_{dyn,X} K_{dyn,I} = K_t(notch) K_{dyn,X}(drop.of.mass) K_{dyn,I}(impulse.force) \Rightarrow Y = 1.2 \cdot 1.5 \cdot 1.2 \approx 2 \tag{23}$$

Thus

$$s_5 = \frac{a_{th0}(im)}{a_0(im)} = \frac{threshold}{existing}, a_0(im) = 0.1mm, \quad 100 < s_5 < 20000 \tag{24}$$

5.4.6 Goal of Obtaining Long Enough Crack Initiation Life

This method of calculating fatigue life N_{life} combines the Haigh diagram of modified Goodman type and the S-N diagram according to (Meyer, 1985), Figure 9.

$$N_{life} = 10^A \quad , \quad A = log\left[\frac{V_a V_e}{(1-V_m)c^2}\right]\left[\frac{3}{log(V_e / c)}\right] \quad , \quad xx(6) = A \tag{25}$$

The decision variable is

$$s_6 = \frac{N_{life}}{10^6} \quad , 2 < s6 < 20000 \quad p_1, p_2 = 0.1, 3 \tag{26}$$

Where three stress ratios are used

$$\sigma_{vm} = Y\sigma_P, \quad Y = 2, \quad \sigma_{va} = 0.4\sigma_{vm}, \quad \Delta\sigma = 2\sigma_{va}, \quad R_m = R_m(im) \tag{27}$$

Thus

$$V_a = \frac{\sigma_{va}}{R_m}, \quad V_m = \frac{\sigma_{vm}}{R_m}, \quad V_e = \frac{S_e}{R_m}, \quad c = 0.9 \tag{28}$$

here V_{a} is relative effective stress amplitude, V_{m} is relative effective mean stress and V_{e} is relative effective corrected fatigue strength. In these

$$\sigma_{\mathrm{vm}} = \left(\sigma_{\mathrm{m}}^2 + 3\tau_{\mathrm{m}}^2\right)^{1/2}, \sigma_{\mathrm{va}} = \left(\sigma_{\mathrm{a}}^2 + 3\tau_{\mathrm{a}}^2\right)^{1/2} \tag{29}$$

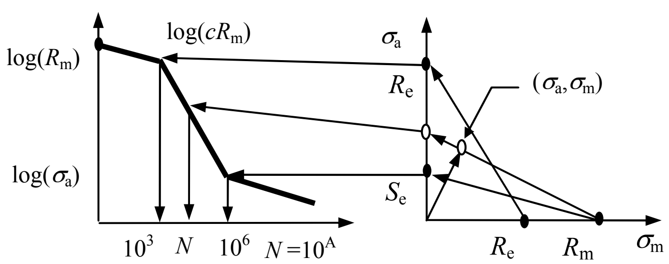

Figure 9. The method of calculating fatigue lives of crack initiation time from normal mean stress and amplitude stress vs. S-N diagram

5.4.7 Goal of Obtaining Satisfactory Fatigue Crack Propagation Life

When the structure contains initial flaws then the fatigue life is about the same as time spent in crack growth since initiation time does not occur. According to (Gurney, 1978) the Paris-Erdogan law is applicable,

$$\frac{da}{dN} = C(\Delta K)^m, \quad \Delta K = Y\Delta\sigma\sqrt{\pi a} \quad , a_f = \frac{1}{\pi}\left(\frac{K_{Ic}}{R_e}\right)^2 \quad \Delta\sigma = \sigma_{max} - \sigma_{min} = 0.2\sigma_P \tag{30}$$

Where

a is crack length, in mm units, ΔK is stress intensity factor range, $\Delta\sigma$ is stress, (MPa).

Y is factor due to geometry close to crack. Now $Y = 2 > 1.2$, at the edge of the holes.

a_{f} is the final crack length, mm, R_{e} is yield strength and K_{Ic} is fracture toughness.

a_0 is initial crack size. It depends on steel strength .For steels with $R_{\mathrm{m}} > 700$, $a_0 = .015$, mm and with $R_{\mathrm{m}} < 700$, $a_0 = 0.05$mm. Now a_0 is estimated conservatively higher, $a_0 = 0.2$mm.

The factor C is estimated according to (Gurney, 1978). In this model the exponent m

$$m = 600\left(R_e\left[Pa\right]\right)^{-0.264}\ C = \frac{A}{B^m} C = C_{corr} C \tag{31}$$

Here the parameters are A=131.5·10^{-6}, B=895.4 at the stress ratio, $R_s=\sigma_{min}/\sigma_{max}=0$, C_{corr} is corrosion enhancement factor. Some rough estimates are: C_{corr}=1 with no corrosion and C_{corr}=10 with wet corrosion.

C_{corr} increases when the surface moisture is increased from dry to 80%. At very low ΔK values C_{corr} is 20 and at high ΔK values it is about 3.

Basic mechanical relationships are illustrated in Figure 10.

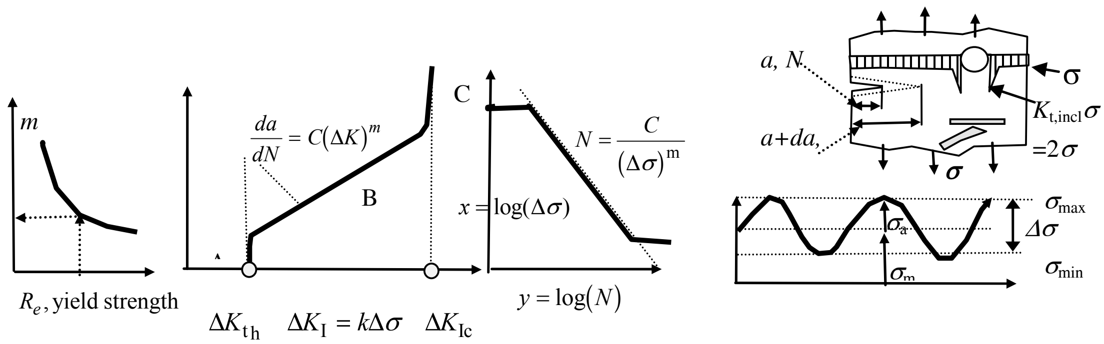

Figure 10. Basic relationships of fracture mechanics

The fatigue life in number of cycles from initial to final crack length is

$$N(im) = \frac{1}{C(im)\left(\frac{1}{2}m(im)-1\right)\left(\Delta\sigma Y\sqrt{\pi}\right)^{m(im)}}\left[\frac{1}{a_0(im)^{\frac{1}{2}m-1}} - \frac{1}{a_f(im)^{\frac{1}{2}m-1}}\right] \tag{32}$$

High enough value is desirable

$$s_7 = \frac{N}{10^6},\quad 0.1 = s_{7\,min} < s_7 < s_{7\,max} = 10000,\quad bias: p_1, p_2 = 0.1, 2 \tag{33}$$

5.4.8 The Goal of Obtaining Satisfactorily Low Creep Rate

Creep occurs in metals. A simple reasonable model is given by (Harris & Evans, 1976), Figure 11.

$$\varepsilon = \varepsilon_0 = const,\quad S = \frac{\sigma - \sigma_0}{\sigma_{0.05}(T)},\quad \dot{\varepsilon} = \dot{\varepsilon}_{el} + \dot{\varepsilon}_s = \frac{1}{E}\frac{d\sigma}{dt} + B\left(\frac{\sigma - \sigma_0}{\sigma_{0.05}}\right)^p = 0 \tag{34}$$

Here σ_0=10 MPa is the creep friction stress. The plastic creep rate is reasonably constant

$$\dot{\varepsilon}_s = B\left(\frac{\sigma - \sigma_0}{\sigma_{0.05}}\right)^p < 10^{-7}, B = 25\cdot 10^{-6},\ p = 3.5,\ \sigma_0 = 10MPa,\ \sigma = \sigma_P \tag{35}$$

Here the yield strength at 0.5% strain and at temperature t is roughly

$$\sigma_{0.05}(T) \approx R_e\left(1 - \frac{t\left[{}^\circ C\right]}{800}\right) \tag{36}$$

The decision variable may be set to

$$s_8 = \frac{\dot{\varepsilon}_s\left[s^{-1}\right]}{10^{-12}\left[s^{-1}\right]}\quad 1 < s_8 < 10\quad p_1, p_2 = 0.1, 1 \tag{37}$$

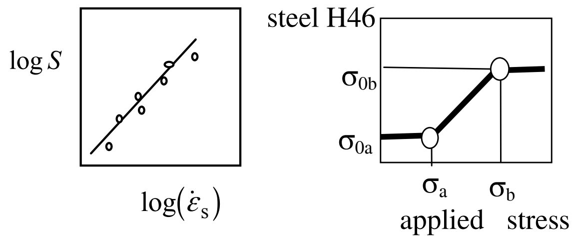

a) b)

Figure 11. Creep models. a) Relative stress S vs. strain rate schematically; b) Friction stress

5.4.9 The Goal of Obtaining Satisfactory Factor of Safety of the Bridge Plate

The maximum bending stress at the bridge plate is decreased by the two P forces, Appendix 1

$$k_1 = 1-\frac{a_1}{L},\quad k_2 = 1-\frac{a_2}{L},\quad Q_{\mathrm{tot}} = Q + m_{\mathrm{B}}g \quad ,P_1 = P_2 = P$$
$$M(x) = -P_1\left(\langle x-a_1\rangle^1 - x\cdot k_1\right) - P_2\left(\langle x-a_2\rangle^1 - x\cdot k_2\right) + \tfrac{1}{2}Q_{\mathrm{tot}}x\left(1-\frac{x}{L}\right) \tag{38}$$

Here Q_{tot} is the total distributed load resultant. Thus at mid

$$M\left(x=\tfrac{1}{2}L\right) = -Pa_1 + \tfrac{1}{8}Q_{\mathrm{tot}}L \tag{39}$$

$$M_{\mathrm{brid}} = M\left(x=\tfrac{1}{2}L\right), \sigma = \frac{M_{\mathrm{brid}}}{W}, W = \frac{I}{\frac{1}{2}D} \tag{40}$$

The decision variable and its parameters are

$$s_9 = N_{\mathrm{b}} = \frac{\sigma_{all}}{\sigma}, 1 < s_9 < 1000 p_1, p_2 = 0.1,2 \tag{41}$$

5.4.10 The Goal of Obtaining Low Enough Sag at the Middle

The allowed sag at the middle is restricted to d_{all} = 0.01 L, Figure 12. At the left side the force P_1 causes deflection curve

$$AC, x < a: d_{P1}(x) = P_1\frac{L^3}{6EI}\left(\frac{a}{L}\frac{b}{L}\right)^2\left(2\frac{x}{a}+\frac{x}{b}-\left(\frac{x}{a}\right)^2\frac{x}{b}\right) \tag{42}$$

At the right side the force P_1 causes deflection curve

$$CB, x > a: d_{P1}(x_1) = P_1\frac{L^3}{6EI}\left(\frac{a}{L}\frac{b}{L}\right)^2\left(2\frac{x_1}{b}+\frac{x_1}{a}-\left(\frac{x_1}{b}\right)^2\frac{x_1}{a}\right) \tag{43}$$

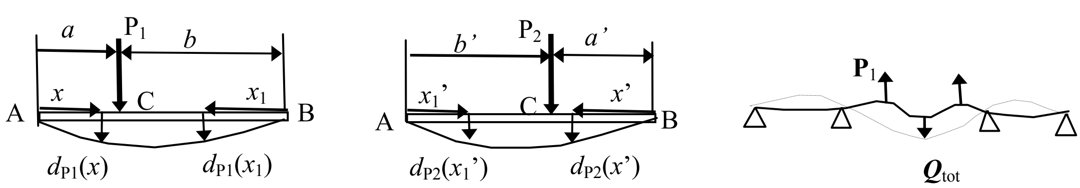

a) b) c)

Figure 12. Deck deflection schematics. a) P_1 force acts; b) P_2 force acts; c) Both forces act

The force P_1 acts at $x= a$ and the deflection to the right of a x> a at $x_1= ½L$ is

$$x > a: d_{P1}\left(x_1=\tfrac{1}{2}L\right) = P_1\frac{L^3}{6EI}\left(\frac{a}{L}\frac{b}{L}\right)^2\left(\frac{L}{b}+\frac{L}{2a}-\left(\frac{L}{2b}\right)^2\frac{L}{2a}\right) = P_1 D \tag{44}$$

The force P_2 acts at $x'=a'$ and the deflection over $x'>a'$ is to the left on P_2

$$x > a : d_{P2}(x_1) = P_2 \frac{L^3}{6EI}\left(\frac{a}{L}\frac{b}{L}\right)^2\left(2\frac{x_1}{b}+\frac{x_1}{a}-\left(\frac{x_1}{b}\right)^2\frac{x_1}{a}\right) \tag{45}$$

The deflection at the middle due to P_2 is obtained with substitutions

$$\begin{aligned} &a \Rightarrow a, b \Rightarrow b, x_1 \Rightarrow \tfrac{1}{2}L \\ &d_{P2}(x_1 = L) = P_2 D \end{aligned} \tag{46}$$

Thus total deflection due to $P_1 = P_2 = P$ is at mid deck

$$d_{2P} = d_{P1} + d_{P2} = 2P \cdot D \tag{47}$$

Deflection to Q loading is

$$d_Q(x=L) = \frac{x_Q}{384}\frac{QL^3}{EI}, \ \textit{simple support} \quad x_Q = 5, \ \textit{stiff support}: x_Q = 1 \tag{48}$$

Now the stiff support model for the mid deck was more realistic .The decision variable is

$$s_{10} = abs\left(\frac{d}{d_{all}}\right) = \frac{d_{2P}+d_Q}{0.01L}, \quad 0.001 < s_{10} < 3 \quad p_1, p_2 = 0.1, 4 \tag{49}$$

5.4.11 The Goal Of Obtaining Desired Factor of Safety Against Flutter Resonance of the Bridge Plate

The mid bridge plate is modelled as a stiffly supported beam, Figure 13.

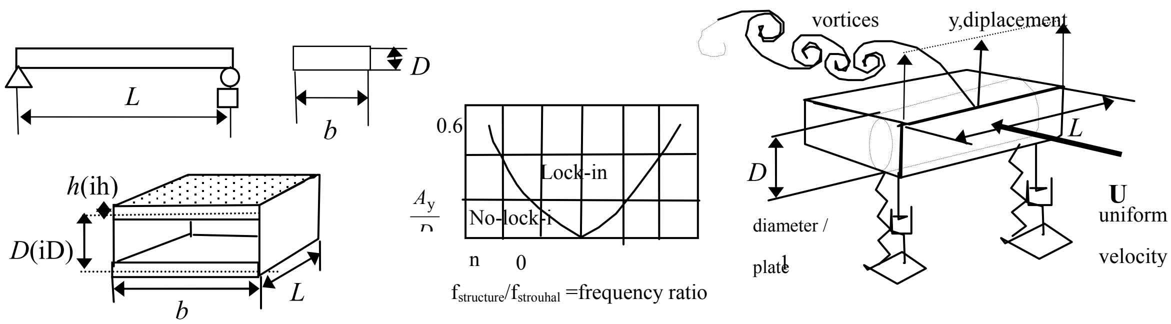

Figure 13. a) beam model for the bridge plate; b) Flutter models

The lowest eigenfrequency of the beam with free supports is

$$\omega_1 = \pi^2\sqrt{\frac{EI}{mL^3}} \tag{50}$$

The orders of magnitude estimates is using the total mass m

$$\begin{aligned} &I = Wz \cdot \tfrac{1}{2}H = \tfrac{1}{6H}\left[B H^3 - b h^3\right] \cdot \tfrac{1}{2}H = 1.02m^4 \\ &B = b, H = D, b = B - 2h, h = H - 2h \end{aligned} \tag{51}$$

Thus the eigenfrequency is

$$\omega_1 = 10\sqrt{\frac{2.05 \cdot 10^{11}\, Pa \cdot 1.02m^4}{\frac{1}{9.81} 2.6 \cdot 10^7\, kg\,(200m)^3}} = 0.32\,\tfrac{rad}{s}, \ f_1 = \frac{\omega_1}{2\pi} = 0.05Hz \tag{52}$$

If external excitation load frequency coincides with this eigenvalue then a flutter induced resonance risk increases. Now the load excitation is due to wind induced flutter vibration at the Strouhal frequency. The annual average wind speed 5 m/s .The wind range is from 0 to 10m/s.

$$f_{str} = \frac{U}{D} = \frac{5\frac{m}{s}}{2m} = 2.5Hz \tag{53}$$

Decision variable is flutter vibration factor of safety

$$s_{11} = N_{\text{str}} = S = \frac{\text{"}strength\text{"}}{\text{"}stress\text{"}} = \frac{f_{\text{structure}}}{f_{\text{strouhal}}} = \frac{f_1}{\frac{U}{D}},\ p_1,\ p_2 = 0.1, 1 \tag{54}$$
$$Range = 0.8 < s_{11} < 1.2\ desirable : P(s_{11}) = 1 - P(Range)$$

FEM results gave that a Tacoma type torsional mode occurs at 2.74Hz. Thus there is a flutter risk.

5.4.12 Goals of Obtaining Other Satisfactions

Goal of obtaining satisfactory ecological value

$$\mathrm{s}_{12} = \mathrm{eco}(\mathrm{im}), 0.05 < \mathrm{s}_{12} < 0.95, \mathrm{p}_1, \mathrm{p}_2 = 0.1, 1 \tag{55}$$

Goal of obtain satisfactory corrosion resistance of material

$$\mathrm{s}_{13} = \mathrm{corres}(\mathrm{im}), 0.05 < \mathrm{s}_{13} < 0.95, \mathrm{p}_1, \mathrm{p}_2 = 0.1, 1 \tag{56}$$

Goal of obtaining aesthetic satisfaction is often imposed on designs.

The bridges are monumental engineering and architectural artefacts which are designed to last for many generations. In this case study the aesthetic impressions id expressed using fuzzy logic very roughly only.

The aesthetic impressions may be costly to realize. Often it is desirable that the ratio *k/L* is close to the golden section

$$\phi^2 = \phi + 1 \Rightarrow \phi = \tfrac{1}{2}\left(1 + \sqrt{5}\right) = 1.618 \tag{57}$$

The range is centred around the maximally aesthetics outlook is

$$s_{14} = \frac{L}{k} = \frac{innerspan}{height.of.pillars}\quad 0.4\varphi < s_{14} < 3\varphi,\ \ p_1, p_2 = 1, 1 \tag{58}$$

Goal of obtaining minimal bending moment at the deck is useful to speed up convergence.

$$s_{15} = \left(\frac{M_{brid}}{M_{max}}\right)^2,\ M_{max} = 10^6\ \ 1 < s15 < 100\ \ p_1, p_2 = 0.1, 4 \tag{59}$$

6. Results of Optimisation

6.1 Results of Analytical Optimisation

Table 4. The most important optimal decision variables and design variables

material im	High strength steel		Low strength steel	
	im=1 OX		im = 2 st52	
Total satisfaction *P* (·scaled)	*P*= 0.146		*P*=0.736	
k = tower height (m)	*k* =45	*k* =20	*k* =45	*k* =20
D = deck plate separation (m)	*D* =1.68	*D* =1.68	*D* =2	*D* =2
h = deck plate thickness (m)	*h* =0.05	*h* =0.05	*h* =0.05	*h* =0.05
a = distance to *P* force	*a* =80	*a* =80	*a* =80	*a* =96
P,T,H forces, (MN)	0.2,1.8,1.8	0.4,4,4	0.2,1.8,1.8	0.2,4.8,4.8
N_{br}, bridge safety factor,σ_{all}	4.5, 1000	4.5, 1000	1.8, 335	1.9,335
Bridge deck stress σ_{br} (MPa)	222	222	183	176
d = deflection at middle (m)	0.12	0.12	0.08	0.04

The allowable static stress $\sigma_{all} = R_e$ is set equal to yield strength.

The stresses in the cables are σ_T, σ_P, σ_H and deck plate stress is σ_{br}.

6.2 Comparison with FEM Results

The main dimensions of the FEM model are set to same as with the optimal result, Figure 14.

$D = 2$, $h = 0.05$ and $k = 45$ and $a = 80$. The low strength steel is used.

The bridge bending stress comparison

- FEM model gave σ_{br} (FEM) = +97/137
- Analytic model gave σ_{br} (anal) = +183/-183

Deck Deflections

The FEM deflection result d(FEM) = 0.388m. This was obtained with realistic support conditions

The analytic deflection result was d(anal) = 0.12 m, assuming stiff support at deck ends

If free support is assumed at the deck ends then the deflection is 5 times higher d' = 1 m

FEM results show that the support is a mixed one end closer to stiff support

Cable Factors of Safety

In FEM calculation cables were wires with E = 150000 MPa and density 4000 kg/m^3.

The cross section area was very large and stresses were low and factors of safety large.

Satisfactions

In optimum the cost was dominant. All the technical requirements were reasonably well satisfied.

The total satisfaction roughly is the same as the cost satisfaction:

P (high strength steel, im = 1, high cost) = 0.146, Cost = 320.

P (low strength steel, im = 2, low cost) = 0.736, Cost = 80.

Final Adjustments by FEM

The final adjustment of topology, geometry and material can be made only after more elaborate specifications and calculations using FEM. But often the final concept decision is made on the basis of cost alone.

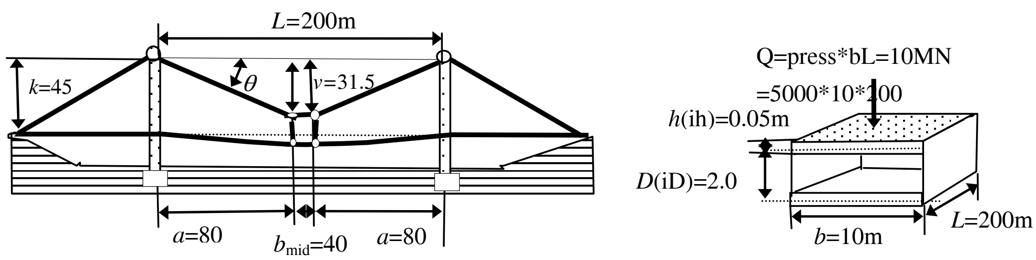

Figure 14. Optimal dimensions for soft steel option

7. FEM Results

The main dimensions of the FEM model are set to the same as with the optimal result

$D = 2$, $h = 0.05$ and $k = 45$. and $a = 80$. The low strength steel is used.

FEM models were made by Erkki Taitokari.

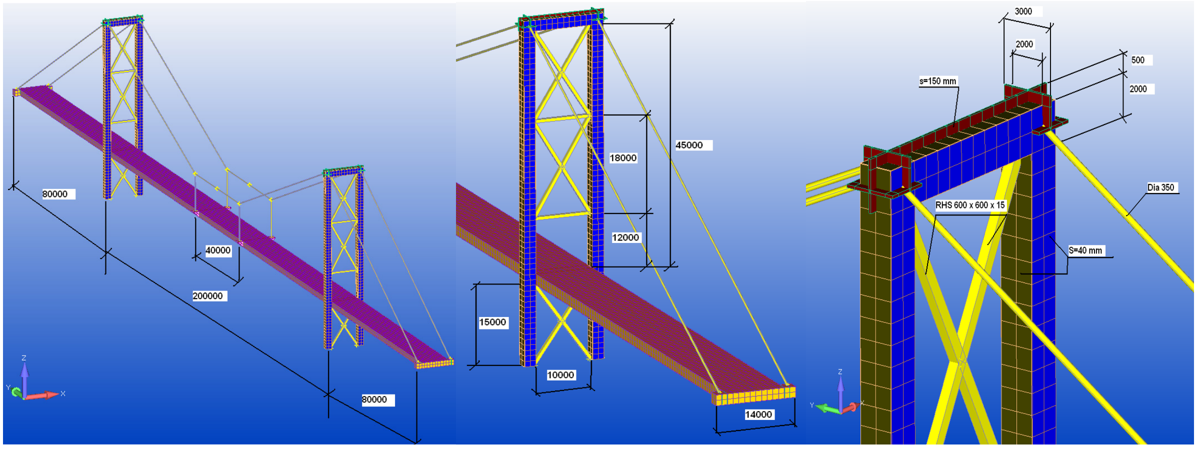

a) b) c)

Figure 15. Bridge FEM model. a) Overall dimensions; b) Vertical frame; c) Details of the top of the vertical frame

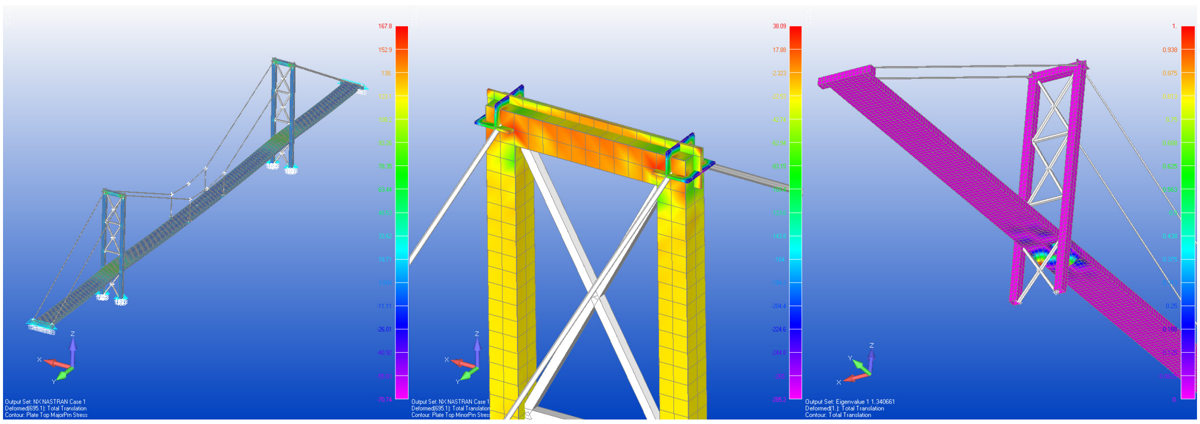

a) b) c)

Figure 16. a) Maximal stresses in the bridge range in +167/-71 MPa; b) The first buckling mode has a safety factor SF = 1.34. The required may be set as 2. In the final designs stiffeners are used at critical locations

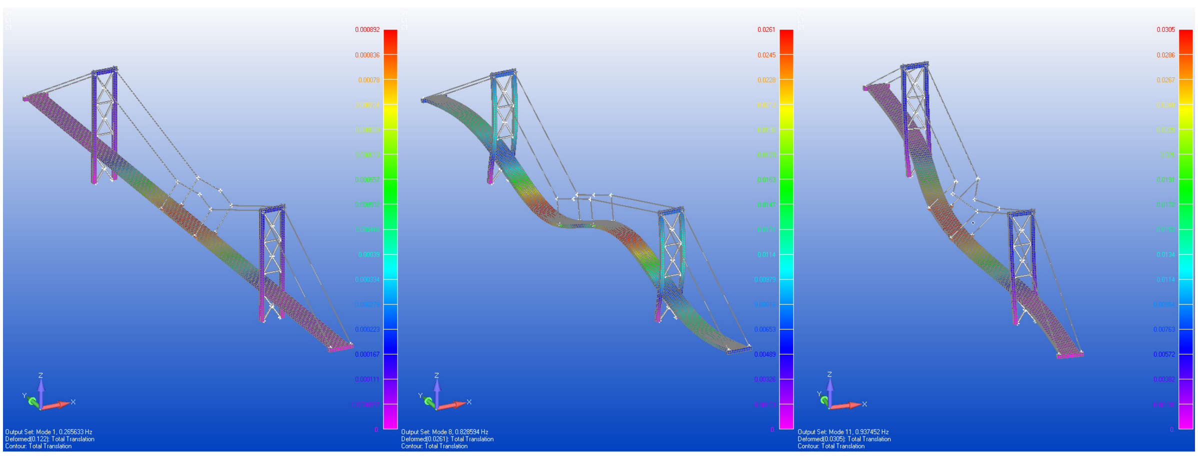

a) b) c)

Figure 17. Lowest eigenfrequencies of the deck. a) f_{1st}(deck) = f_1= 0.265 Hz; b) the second lowest is f_{2nd} (deck) = f_8 = 0.829 Hz. The modes of the intermediate frequencies f_2 to f_7 are cable spring vibrations; c) The third deck eigenfrequency f_{3rd}(deck)= f_{11}=0.937Hz. The intermediate f_9, f_{10} are cable vibrations

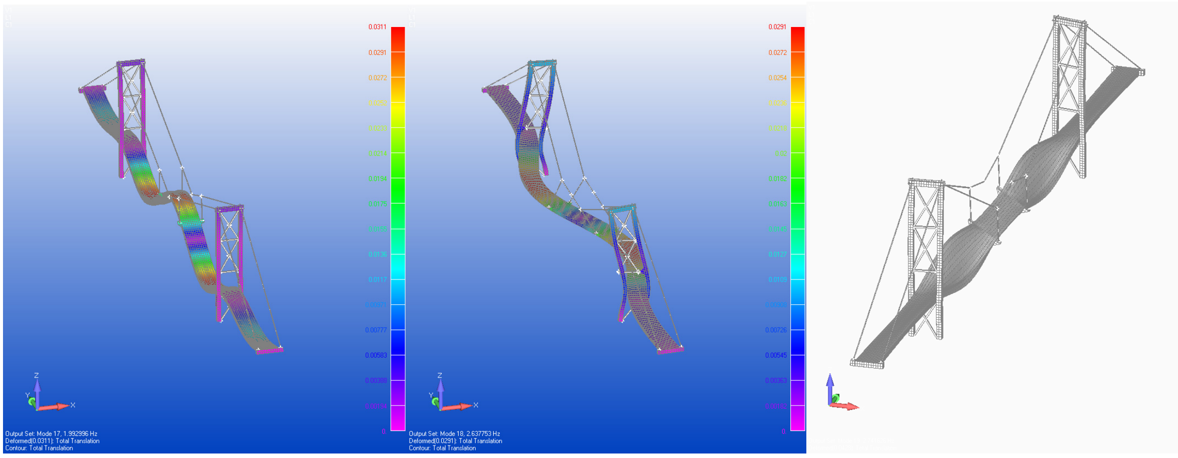

a) b) c)

Figure 18. Bridge vibrations. a) frequency f_{17}=1.99Hz with sinusoidal wave forms; b) f_{18} = 2.64Hz, Sideways motion of deck with bending of the supports; c) Torsional vibration with f=2.74 Hz. This is similar to the Tacoma Narrows Bridge vibration before failure. Strouhal vibrations with frequency f= U/D=5(m/s) /2m =2.5Hz may occur with wind speed U= 5m/s

8. Conclusions

The main conclusions of the present study can be summarised as follows

8.1 This study is Motivated by the Observed Megatrend of Rising Need for Bridging

Bridging is needed over a physical chasm in an area using new innovative solutions. A short survey of history shows that the suspension bridge has been a successful solution although with some failures. The aim is to find out what can be learnt from their design and utilisation history. Traditionally the main need has been to get a safe and low cost passage over some chasm. Many present day basic bridge concepts have been invented and realised successfully already even some 4000 years ago. The design and construction methods of ancients are not known to us.

8.2 The Study Shows that the Modern Method Can be Used to "re invent" Old Inventions

We can and also learn from past failures to enhance the probability of success in our designs and avoid repeating failures. One finding of this study is that the design loop and the fault tree methods are powerful to increase innovations and their reliability.

8.3 The aim of This Study was to Check the Cost Effectiveness of Combining Two Methods in this Case Study

This first method is fuzzy optimum design and it is used to get the best concept for further design.

The second method is to use FEM to fine tune and check the structural behaviour of the design concept.

The third stage would be design for manufacturability. Now it was beyond the scope. One trend is to obtain an all encompassing optimum design, product and manufacturing design methodology.

8.4 The Initial Optimal Concept is Obtained Effectively Using the Heuristics Fuzzy Optimum Design

- At the first basic level engineering mechanics is used. to define the design variables for all relevant functional geometric and material aspects of the object
- At the next more abstract level the decision variables are defined based on design variables. Among them are total cost, factors of safety, reliability and ecology.
- At the third abstraction level the fuzzy psychological satisfaction of the end user on the final concept is measured. Total satisfaction is measured as the product of partial satisfactions on each decision variable.

The case study was a steel suspension bridge. One optimal trade-off concept was obtained. Optimality of the concept changes depending on the wishes of the end user.

8.5 The Power of FEM is Essential to Fine Tune and Check the Optimal Concept

FE method was applied to analyse the static, dynamic and buckling behaviour of the optimal concept.

The structural details were added and dynamic behaviour was obtained. This revealed an aero elastic flutter risk at average wind speed, buckling overloading and resonance risks. FEM is a powerful tool to minimise these risks and ensure the optimality of the design by fine tuning the structural details and also the overall model.

8.6 A New Visionary Design Approach is Promising along the Ecological Megatrend

This study emphasises the emerging need that the utility of bridges to the society should be increased due to the high investment costs of bridges. Traditional goal is the narrow utilitarian aim the make a bridging and collect taxes. Bridge taxes should be levied also from the environment. The old design goal was only to passively resist at the cost of bridge endurance all kinds of energy flows from winds to water flow below and solar radiation and mechanical vibrations. These energy flows may be harvested and converted to produce ecologically electric energy for the bridge maintenance and the society. Since there are many bridges the total obtained power may be high

References

Ackermann, T., & Söder, L. (2000). Wind energy technology and current status: a Review. *Renewable and Sustainable Energy Reviews, 4*, 315-374. http://dx.doi.org/10.1016/S1364-0321(00)00004-6

Blevins, R. D. (1990). *Flow-induced Vibrations*. Van Nostrand Reinhold.

Boresi, A., Schmidt, R., & Sidebottom, O. (1993). *Advanced mechanics of materials*. John Wiley.

Brooklyn Bridge. Retrieved from http://www.greatbuildings/Brooklyn_Bridge.html

Brown, D. J. (2005). *Bridges: Three Thousand Years of Defying Nature*. Richmond Hill, Ont: Firefly Books.

Cable-Stayed Bridges. Retrived from http://en.wikipedia.org/wiki/Cable-stayed_bridge

Case, J., Lord Chilver, Carl, & Ross, C. F. T. (1993). *Strength of materials and structures with an introduction to finite element methods*. Edward Arnold.

Chiaopas. Retrieved from http://www.thesavvyexplorer.com/index.php/foodsteps-history/32-history-article/644-chiaopas-and-the-mayans?start=3

Dhillon, B. S., & Singh, C. (1981). *Enginering Reliability*. Wiley-Interscience.

Diaz, A. (1988). Goal aggregation in design optimization. *Engineering Optimization, 13*, 257-273. http://dx.doi.org/10.1080/03052158808940958

Dimarogonas, A. D., & Haddad, S. (1992). *Vibration for Engineers*. Prentice Hall.

Evans, W. J., & Harrison, G. F. (1976). The development of a universal equation for secondary creep rates in pure metals and engineering alloys. *Metal Science*, 307-313.

Goldsmith, W. (2001). *Impact. The Theory and Physical Behavior of Colliding Solids*. Dover Publications Inc.

Gurney, T. R. (1978). An analysis of some crack propagation data for steel subjected to pulsating tension loading. *The Welding Institute*, 59/1978/E.

Leitch, R. D. (1988). Basic reliability engineering analysis, Butterworths, London

Martikka, H., & Pöllänen, I. (2009). Multi-objective optimisation by technical laws and heuristics. *Memetic Computing*. http://dx.doi.org/10.1007/s12293-009-0007-x

Merritt, F. S. (1983). *Standard Handbook for Civil Engineers*. McGraw-Hill, Inc.

Meyer, J. A. (1985). Finite life under combined stress, *Machine Design*, August, 83-84.

NX Nastran FEM program.

Szilard, R. (1975). *Theory and Analysis of Plates*. Prentice-Hall

Tacoma Narrows Bridge. Retrieved from http:// en.wikipedia.org/wiki/Tacoma_Narrws_Bridge_%281940%29

Ventsel, E., & Krauthammer, T. (2001). *Thin Plates and shells*. New York, NY: Marcel Dekker. http://dx.doi.org/10.1201/9780203908723

Yaxchilan. Retrieved from http://www.panoramio.com/photo/1734120

Appendix 1. Derivation of the Moments at the Bridge Plate and Its Deflection

The following simplifying and conservative assumption is first made.

The deck beam is freely supported at the ends $x = 0$ and $x = L$.

Actually it is an inseminate beam and the support is closer to stiff support.

The maximum bending stress and deflection at the bridge plate is decreased by the two P forces.

First a short derivation is reviewed.

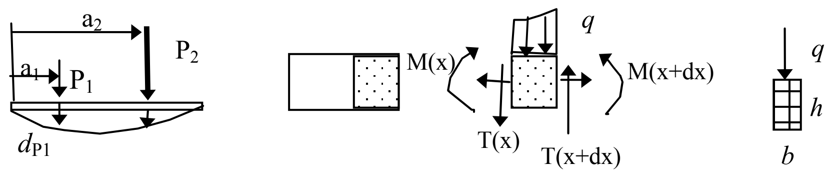

Figure A1-1. a) Deck model; b) Beam model and free body element

First the free body balance of a beam element gives for the N, T and M dependence on the line load q, $q = pb$, b is width of the beam and p is pressure on it.

Loads on the beam are calculated using equations, (Case, 1999)

$$\frac{dN}{dx} = 0 \quad , \quad \frac{dT}{dx} = -q \quad , \quad \frac{dM}{dx} = T \tag{A1-1}$$

The sign assumptions are that P forces act down.

$$q = -P\langle x-a\rangle_{-1} - \left[pb\langle x-x_1\rangle^0 - pb\langle x-x_2\rangle^0\right] + A\langle x-0\rangle_{-1} + B\langle x-L\rangle_{-1} \tag{A1-2}$$

Integration of this over the beam gives force load on the beam

$$\int_0^L q dx = \left[-P\langle x-a\rangle^0 - \left[pb\langle x-x_1\rangle^1 - pb\langle x-x_2\rangle^1\right] + A\langle x-0\rangle^0 + B\langle x-L\rangle^0\right]_0^L \Rightarrow 0 \tag{A1-3}$$

Thus

$$\int_0^L q dx = \left[-P\langle L-a\rangle^0 - \left[pb\langle L-x_1\rangle^1 - pb\langle L-x_2\rangle^1\right] + A\langle L-0\rangle^0 + B\langle L_+ - L\rangle^0\right] \Rightarrow 0 \tag{A1-4}$$

This is the force balance

$$\Sigma F = -P - \left[pb(x_2 - x_1)\right] + A + B = 0 \tag{A1-5}$$

The sum force at section x

$$\int_0^x q dx = -\int_0^x \frac{dT}{dx} dx = -T(x) = \left[-P\langle x-a\rangle^0 - \left[pb\langle x-x_1\rangle^1 - pb\langle x-x_2\rangle^1\right] + A\langle x-0\rangle^0 + B\langle x-L\rangle^0\right]_0^x \tag{A1-6}$$

Here

$$B\langle x-L<0\rangle^0 = 0 \tag{A1-7}$$

Thus

$$M(x) = \int_0^x T(x)dx = \int_0^x \left[+P\langle x-a\rangle^0 + \left[pb\langle x-x_1\rangle^1 - pb\langle x-x_2\rangle^1\right] - A\langle x-0\rangle^0\right] dx \tag{A1-8}$$

The moment is

$$M(x) = -P\langle x-a\rangle^1 - \tfrac{1}{2}\left[pb\langle x-x_1\rangle^2 - pb\langle x-x_2\rangle^2\right] + A\langle x-0\rangle^1 \tag{A1-9}$$

Use is made of integral

$$\int_{-\infty}^{X} \langle x-a\rangle^{\mathrm{n}} dx = \int_{a^+}^{X} (x-a)^{\mathrm{n}} dx = \frac{(X-a)^{\mathrm{n}}}{n+1} \quad , \langle X\rangle = X, if \quad X>0, \quad else \quad 0 \tag{A1-10}$$

The case of continuous loading Q only over the whole beam and P is zero.

In this case the force P are zero and only Q acts

$$P = 0, \quad x_1 = 0, x_2 = L, Q = pbL, \quad A = B = \tfrac{1}{2}Q \tag{A1-11}$$

Thus

$$M_{\mathrm{Q}}(x) = -\tfrac{1}{2}\left[\frac{Q}{L}\rangle x-0\langle^2 - \frac{Q}{L}\rangle x-L\langle^2\right] + \tfrac{1}{2}Qx = \tfrac{1}{2}Qx\left(1-\frac{x}{L}\right) \tag{A1-12}$$

The case when both Q and P forces act

The support reactions A and B are produced by Q and P

$$M(x) = -P\langle x-a\rangle^1 - \tfrac{1}{2}pb\langle x-0\rangle^2 + A\langle x-0\rangle^1 \tag{A1-13}$$

At the end $x = L$ the moment is zero

$$M(L) = -P\langle L-a\rangle^1 - \tfrac{1}{2}pb\langle L-0\rangle^2 + A\langle L-0\rangle^1 = 0 \tag{A1-14}$$

From this the support reaction is obtained

$$A = P\left(1-\frac{a}{L}\right) + \tfrac{1}{2}pbL = Pk + \tfrac{1}{2}Q \tag{A1-15}$$

Thus

$$Q = pbL, \quad k = 1-\frac{a}{L} \quad , \quad M(x) = -P\left(\langle x-a\rangle^1 - xk\right) + \tfrac{1}{2}Qx\left(1-\frac{x}{L}\right) \tag{A1-16}$$

Bending moment of two force P_1 and P_2 and Q

$$k_1 = 1-\frac{a_1}{L} \quad , \quad k_2 = 1-\frac{a_2}{L} \tag{A1-17}$$

$$M(x) = -P_1\left(\langle x-a_1\rangle^1 - x\cdot k_1\right) - P_2\left(\langle x-a_2\rangle^1 - x\cdot k_2\right) + \tfrac{1}{2}Qx\left(1-\frac{x}{L}\right) \tag{A1-18}$$

Now the bridge is symmetric at middle section

$$P_1 = P_2 = P$$

The maximum bending stress occurs at the middle

$$M\left(\tfrac{1}{2}L\right) = -P_1\left(\left\langle \tfrac{1}{2}L - a_1 > 0\right\rangle^1 - \tfrac{1}{2}L\cdot k_1\right) - P_2\left(\left\langle \tfrac{1}{2}L - a_2 < \tfrac{1}{2}L\right\rangle^1 - \tfrac{1}{2}L\cdot k_2\right) + \tfrac{1}{2}Q\tfrac{1}{2}L\left(1-\frac{\tfrac{1}{2}L}{L}\right) \tag{A1-19}$$

Thus

$$\begin{gathered} M\left(\tfrac{1}{2}L\right) = -P_1\tfrac{1}{2}\left(L-2a_1 - L\cdot k_1 - Lk_2\right) + \tfrac{1}{8}QL \\ k_1 = 1-\frac{a_1}{L}, k_2 = 1-\frac{a_2}{L}, a_2 = L-a_1 \end{gathered} \tag{A1-20}$$

Thus

$$M\left(\tfrac{1}{2}L\right) = M_{\mathrm{brid}} = -Pa_1 + \tfrac{1}{8}QL \tag{A1-21}$$

The total deflection at support location can be made either using the Castigliano's theorem or by the conventional method of differential equations with solutions in handbooks.

$$d = \frac{\partial}{\partial P}U = \frac{1}{EI}\int_{z=0}^{z=L} M(z)\frac{\partial M}{\partial P}dz \tag{A1-22}$$

Appendix 2. Total Dynamic Load Factor Y

Stress may be locally high due to several causes. This is discussed by (Goldsmith, 2001)

Large dynamic forces may occur on bridges due to dropping of large masses at accidents.

Dynamic stresses cause fatigue and plastic deformations.

$$\sigma(t) = \frac{F(t)}{A} = \frac{F_{\mathrm{m}} + F_{\mathrm{a}} \sin(\Omega t)}{A} \quad , \quad \sigma_{\max} = K_{\mathrm{t}} K_{\mathrm{dyn,M}} K_{\mathrm{dyn,I}} \sigma \tag{A2-1}$$

Here, K_{t} is tensile stress notch concentration. The notch factor may be simplifies roughly as using a stepped plate under tension

$$K_t(notch) = 1 + \frac{1}{G} = 1 + \sqrt{\frac{a}{\rho}} \tag{A2-2}$$

$K_{\mathrm{dyn,I}}$ is due to impulse force , approximately 1...2.

$K_{\mathrm{dyn,M}}$ is due to two mass drop system. In it a mass m_2 is dropped on spring with mass m_1. The mass of the dropped and also the spring mass are considered

$$K_{\mathrm{dyn,M}} = \frac{\sigma_{\mathrm{dyn,max}}}{\sigma_{\mathrm{staat}}} = \frac{EA}{mg} \frac{\frac{v_0}{c}}{\sqrt{M\left(1+\frac{3}{M}\right)}}, \; M = \frac{m_1}{m_2}, \; c = \sqrt{\frac{E}{\rho}} = \sqrt{\frac{2.05 \cdot 10^{11}}{7850}} = 5172 \tfrac{m}{s} \tag{A2-3}$$

Here a is half width of a surrogate plate and ρ is notch root radius of curvature.

The stress increasing factor may come from many sources ant they may be superposed

$$\begin{aligned} Y &= K_{\mathrm{t}} K_{\mathrm{dyn,M}} K_{\mathrm{dyn,I}} = K_{\mathrm{t}}(notch) K_{\mathrm{dyn,X}}(drop.of.mass) K_{\mathrm{dyn,I}}(impulse.force) \\ Y &= 1.2 \cdot 1.5 \cdot 1.2 = 2 \end{aligned} \tag{A2-4}$$

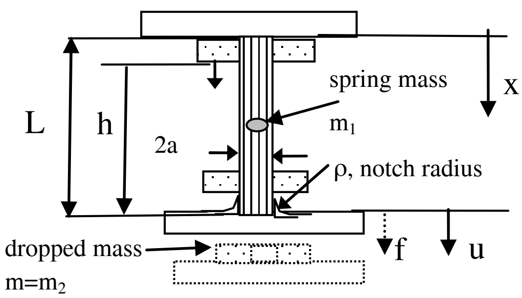

Figure A2-1. Dynamic loading

Appendix 3. Fuzzy and Probabilistic Modelling

A3.1 The Relationship between Fuzzy Modelling and Probabilistic Modelling

The principle is illustrated in Figure A3-1. Two models may be presented

A. Product Model

The satisfaction function is product or two probabilities.

$$P(s) = F_1(s)[1 - F_2(s)] \tag{A3-1}$$

B. Sum Model

Another formulation is interpreted differently

$$P(s) = F_1(s) - F_2(s) \tag{A3-2}$$

Equating these gives the range where they are numerically equal

$$F_1(s)[1-F_2(s)]=F_1(s)-F_2(s)\Rightarrow F_2(s)[1-F_1(s)]=0 \tag{A3-3}$$

Thus

$$\begin{aligned}&solution\ \ 1:\ \ F_2(s)=0\quad and\quad 1\geq F_1(s)\\&solution\ \ 2:\ \ F_2(s)\neq 0\quad 0<F_2(s)\leq 1\quad and\quad 1=F_1(s)\end{aligned} \tag{A3-4}$$

These are shown in Figure A3-1.

These definitions are equal only within the following range of zero P discrepancy

A3.2 The Product Model

The left function

$$F_1(s)=\Pr\{S\leq s\}=\int_{-\infty}^{s} f_1(S)dS \tag{A3-5}$$

The right function

$$1-F_2(s)=1-\Pr\{S'\leq s\}=\Pr\{s>S'\}=1-\int_{-\infty}^{s} f_2(S')dS'=\int_{s}^{\infty} f_2(S')dS' \tag{A3-6}$$

The product of theses gives probability of how well the desirable range is covered by s

$$\begin{aligned}&P(s)=F_1(s)[1-F_{2'}(s)]=\Pr\{S\leq s\}\Pr\{s\leq S'\}=\Pr\{S\leq s\quad AND\quad s\leq S'\}\\&P(s)=\Pr\{S\leq s\leq S'\}\end{aligned} \tag{A3-7}$$

A3.3 Low Satisfaction Desired Within a Range of a Decision Variable

It is often desirable to avoid certain range of decision variables as shown in Figure A3-1

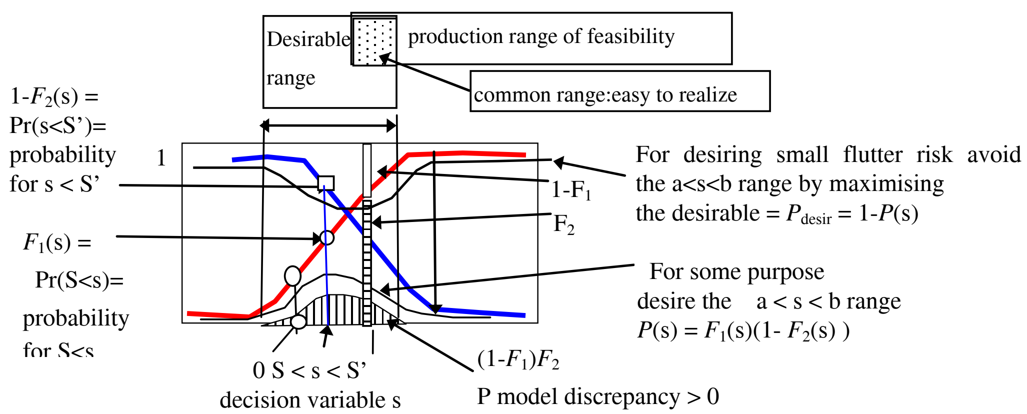

Figure A3-1. Low satisfaction in a range, like Strouhal locking range
Inducing risk of dangerous aero-elastic flutter to the bridge

A3.4 High Satisfaction is Desired within a Range of a Decision Variable

A maximal unity satisfaction is now desired within a range a<s<b. It is realised as shown in Figure A3-2

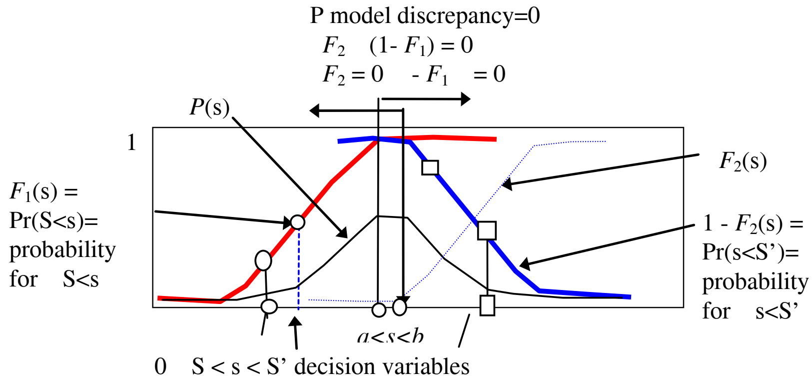

Figure A3-2. Left and right requirements give high satisfaction at a middle range a<s<b

A3.5 Mechanical Spring Model for Describing the Function of the Fuzzy Driving Design Goal

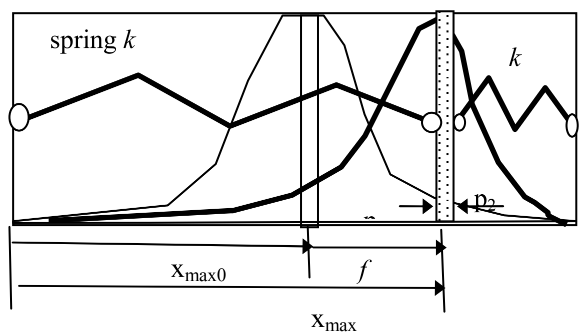

Figure A3-3. A mechanical spring model for describing the function of the fuzzy driving design goal

Force balance on the fictive piston slider

$$(p_1 - p_2)A = 2kf = 2k(x_{max} - x_{max\,0}) \tag{A3-9}$$

Here x_{max} is the peak value of the satisfaction function. It is value at $P(x_{max}) = 1$ unity.

Here p_1 and p_2 are biases. They are analogous to pressures on a piston joined to two springs.

- The spring force describes the fuzzy conservative resistance to changes of "good already" design.
- The pressure force is analogous to drive to radical changes 'paradigms' of design

$$x_{max} = \frac{p_1}{p_1 + p_2}, \quad x_{max\,0} = 0.5 \tag{A3-10}$$

Substituting this gives the news peaks position and the shift f

$$\begin{aligned} & p_1 + p_2 = \frac{k}{A},\ p_1 A = kx_{max} \Rightarrow x_{max} = \frac{p_1 A}{k} \\ & f = x_{max} - x_{max,0} = \frac{(p_1 - p_{1,0})A}{k} \end{aligned} \tag{A3-11}$$

Appendix 4. Algorithm for Optimisation

In engineering optimisation at concept stage most tasks are highly non-linear and also the design variables are few and discrete. User can select the materials from the list of available selections by index.

Total satisfaction is first initialised to a low value to start the algorithm P_{gbest} = .0000001.

Material class selection is made im = 1 or 2.

FOR iP = iP1 TO iP2	PP = PP(iP)’	P =xp*PP = Force in P cable
FOR iA = iA1 TO iA2	AA = AA(iA)	A= xa*AA = cross sectional area of cables ,
FOR iaapL = i1 TO i2	aapL = aapL(iaapL)	a = aapL * L = distence from towers
FOR ivpk = i1 TO i2	vpk = vpk(ivpk)	vpk = v/k = ratio of v and k
FOR ikpL = ikpL1 TO i2	kpL = kpL(ikpL):	k = kpL * L --> v = vpk * k, k= tower height
FOR ih = ih1 TO ih2	hh = hh(ih)	h= xh*hh= thickness of deck plates
FOR iD = iD1 TO iD2	DD= DD(iD)	D= xD*DD= separation of deck plates

For each k = 1, 2...15 decision variable s(k), the desirable range s_1,s_2 and bias definition p_1 and p_2.

Then the satisfaction function $P(s)$ is obtained by a call:

CALL pzz(s_1, s_2, p_1, p_2, s, $P(s)$)

The output is $P(s)$

The total satisfaction is product of partial satisfactions

P_s = 1, the initialisation first, before the loop

FOR i = 1 TO NPs = number of satisfaction functions

Ps = Ps * Ps(i)

NEXT i

$P_g = P_s$

IF $P_g > P_{gbest}$ THEN

' new optimum is found better than previous

ELSE search is continued. END IF

NEXT indices